



Effect of pin penetration depth on double-sided friction stir welded joints of AA6061-T913 alloy

Iman HEJAZI, Seyyed Ehsan MIRSALEHI

Department of Mining and Metallurgical Engineering, Amirkabir University of Technology (Tehran Polytechnic),
424 Hafez Ave, P. O. Box 15875-4413, Tehran, Iran

Received 12 April 2015; accepted 12 October 2015

Abstract: Friction stir welding (FSW) of aluminum alloys is currently utilized in several modern industries. The joints must have sufficient elastic–plastic response and formability levels similar to that of the base metal. In this work, double-sided FSW of AA6061 sheet was compared with its conventional single-sided one. An adjustable tool with different pin lengths (50%–95% of the sheet thickness) was used to perform the double-sided welds. Macro- and micro-structures, strength, and hardness of the joints were investigated to determine the optimum pin penetration depth. The best results were obtained for a double-sided joint made by a pin length equal to 65% of the sheet thickness, which showed an increase of 41% in the ultimate tensile strength compared with the single-sided joint.

Key words: AA6061 aluminium alloy; friction stir welding; double-sided joint; pin length; mechanical properties; microstructure

1 Introduction

Obtaining light, sound and strong joints always has a great interest for scientists and engineers. Apart from the demands in reduction of the mass and cost of metal production, however, researchers are always looking for stronger weld joints. In recent years, the demands for aluminum alloy 6061 have steadily increased in aerospace, aircraft and automotive applications because of its high specific strength, good ductility and corrosion and cracking resistance in adverse environments [1,2]. The increasing relevance of aluminum alloys in transportation requires research on more efficient and reliable joining processes [2]. Friction stir welding (FSW) is a solid-state joining process using frictional and adiabatic heat, generated by a rotating and traversing cylindrical tool with a profiled pin along a weld joint [3]. The FSW was first developed in 1991 by the Welding Institute (TWI) in the United Kingdom, and ever since, this method has gathered a great amount of interest in a variety of applications [4]. FSW was initially applied to aluminum alloys and later, it was used for the welding of a wide variety of metallic materials such as copper and steel [5]. Low distortion, high quality, lower residual stresses, few weld defects, and low cost joints are the

main advantages of this method [6].

Previous studies showed that the double-sided FSW has a great potential to increase strength of the joints [7–11]. There are two possible methods to perform double-sided FSW. The first method is to use a bobbin tool as an alternative tool design. There is a class of FSW tools called bobbin tools (sometimes referred to as self-reacting tools). The name refers to the shape of these tools that consist of two shoulders connected by the tool pin [12]. When a bobbin type tool is used, there is no need for a backing plate, but it is hard to use this tool under the condition that there is limited access to the back of the weldment. The second method is to use two conventional FSW welds on both sides.

The majority of previous studies in double-sided FSW primarily discussed the tool shape and welding parameters except the pin penetration. Some studies reported the relationship between welding parameters and mechanical properties of the double-sided welds. ROHILLA and KUMAR [9] investigated the effect of welding parameters and direction of welding on tensile properties of the joints in a friction stir (FS) welded AA1100. According to their research, double-sided same direction welds are superior in strength compared with opposite directional welds.

Some researchers investigated the effect of FSW

tool geometry on AA6061 weldments [8–10]. The test results show that a sound weld can be obtained using the FSW tool that has a concave shoulder with a diameter approximately equal to four times the welded plate thickness and a tapered cone pin with a base diameter equal to the plate thickness. The pin angle and the shoulder concavity angle should be 20° and 12°, respectively. SINGH et al [11] compared single- and double-sided FSW joints of AA6061. They concluded that the mechanical properties of double-sided welds were improved under specific welding parameters. However, they did not describe a clear relation between the welding parameters and mechanical properties.

The present investigation focused on finding the optimal pin length in double-sided FSW with respect to mechanical properties such as hardness and tensile strength.

2 Experimental

2.1 Materials and welding conditions

Sheets of AA6061-T913 with dimensions of 200 mm × 300 mm × 4 mm were welded by a FSW machine under six different conditions. Chemical composition and mechanical properties of the sheets are shown in Tables 1 and 2, respectively. A special tool with adjustable pin length was fabricated and used. Figure 1 illustrates a basic description of the welding conditions. According to this figure, advancing side (AS) of the first welding side is equivalent to retreating side (RS) of the second welding side.

Table 1 Chemical composition of base metal (mass fraction, %)

Mg	Mn	Fe	Si	Cu	Al
0.89	0.04	0.37	0.64	0.20	Bal.

Table 2 Mechanical properties of base metal

Material	YS/MPa	UTS/MPa	El/%	Hardness (HV)
AA6061-T913	455	460	10	139

YS: Yield strength; UTS: Ultimate tensile strength; El: Elongation (average of three values)

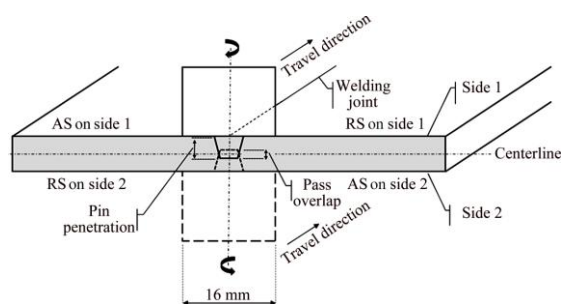


Fig. 1 Schematic diagram showing positions of FSW tool and pin penetration on both sides for experimental set-up and weld configuration

The material of the FSW tool was H13 tool steel. It was subjected to heat treatment to improve its hardness. Its hardness after heat treatment was about HRC 54. The tool had a concave shoulder with a diameter of 16 mm and a tapered cone pin with a base diameter of 4 mm. The pin and shoulder concavity angles were 20° and 12°, respectively. Figure 2 shows a representation of the used tool.

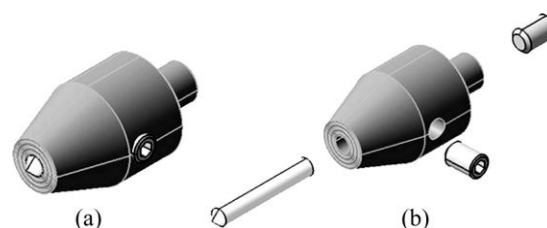


Fig. 2 Schematic representation of assembled (a) and unassembled (b) adjustable FSW tool (Length of pin can be adjusted to desired value by means of side and internal screws. The pin is removable and can be replaced by other types)

In this work, six experiments were performed. During all the experiments, welding parameters except the pin length remained constant. The pin lengths in the six experiments were 2.0, 2.6, 3.0, 3.4, 3.8 and 3.8 mm (50%, 65%, 75%, 85% and 95% of the sheet thickness in double-sided and 95% of the sheet in single-sided welds, respectively). The welding parameters are shown in Table 3.

Table 3 Welding parameters of FSW samples

Sample No.	Sample ID	Type of weld	Pin penetration/ %	Pin length/ mm	Overlap in passes/mm (percentage)
1	D50	Double	50	2.0	0 (0)
2	D65	Double	65	2.6	0.6 (15%)
3	D75	Double	75	3.0	1.0 (25%)
4	D85	Double	85	3.4	1.4 (35%)
5	D95	Double	95	3.8	1.8 (45%)
6	S95	Single	95	3.8	

Rotational speed, ω , 940 r/min; traverse velocity, v , 18 mm/min; plunge (1 mm) and tilt angle (1°) remained constant in all samples

2.2 Mechanical testing

The welds were tested for their mechanical strength and hardness. The main objectives of the tests were to find out the most efficient pin length and penetration for the maximum strength and hardness.

Zwick/SP1200 universal testing machine was used to perform the tensile test of the specimens at a cross-head speed of 1 mm/min. The starting and ending portions of the weld were not used. The tensile specimens were prepared according to standard ASTM E8/E8M [13].

Using Vickers hardness testing machine, hardness across the welds cross-section was measured. Hardness values were taken from weld face, midway through the weld nugget and near the centerline of the FSW joint in accordance with ASTM E384 [14] using an indenter with a load of 0.490 N for a dwell period of 5 s.

2.3 Microstructural observation

Optical microscopy (OM) of the welded joints was carried out using an Olympus B202 microscope, and the microphotographs were taken at different magnifications. For metallurgical investigations, the specimens were prepared according to the ASTM E3–01 [15]. Sample surfaces were polished and etched for a few seconds, using a Weck's reagent consisting of water (100 mL), KMnO_4 (4 g) and NaOH (1 g).

A Philips XL30 scanning electron microscope (SEM), operated at 25 kV, was utilized to investigate the fracture surfaces.

The mean grain sizes were determined by the line intercept method according to the ASTM E112 [16].

3 Results and discussion

As observed in Fig. 3, all the six samples had sound and defect-free welds. Figure 4 illustrates the ultimate tensile strengths of the six FS welded joints, which were made under different pin lengths. The tensile strength increases significantly when the pin length increases from 2.0 to 2.6 mm at given welding parameters (Samples D50 and D65, respectively). According to Fig. 4, Sample D65 has the highest UTS of 226.649 MPa which is 41% greater than that of Sample S95. The appearance of the fracture in the tensile specimens (Fig. 5) indicates that the fracture location in Sample D50 is not far from the weld center, and the fracture occurred in stir zone (SZ). However, tensile fracture in Sample D65 occurred in thermo-mechanically affected zone (TMAZ) near its interface with the heat affected zone (HAZ) in the AS of the first welding side. As the pin length increased (the samples D75 to D95), the fracture location of the joints moved from TMAZ to SZ again.

Figures 6(a)–(d) compare the stir zone microstructures for Samples D50 to D85. According to these figures, it is apparent that Sample D50 has the smallest grain size (Fig. 6(a)) and increasing the pin length has resulted in larger grains in other samples. The variation of tensile strength with length of the pin for given welding parameters appears to be linked to the energy of the welds [17]. Frictional heat is generated between the wear resistant welding tool and the material of the workpieces [18]. The amount of heat generated in combination of the sticking (Q_{sticking}) and sliding (Q_{sliding}) states is [19]

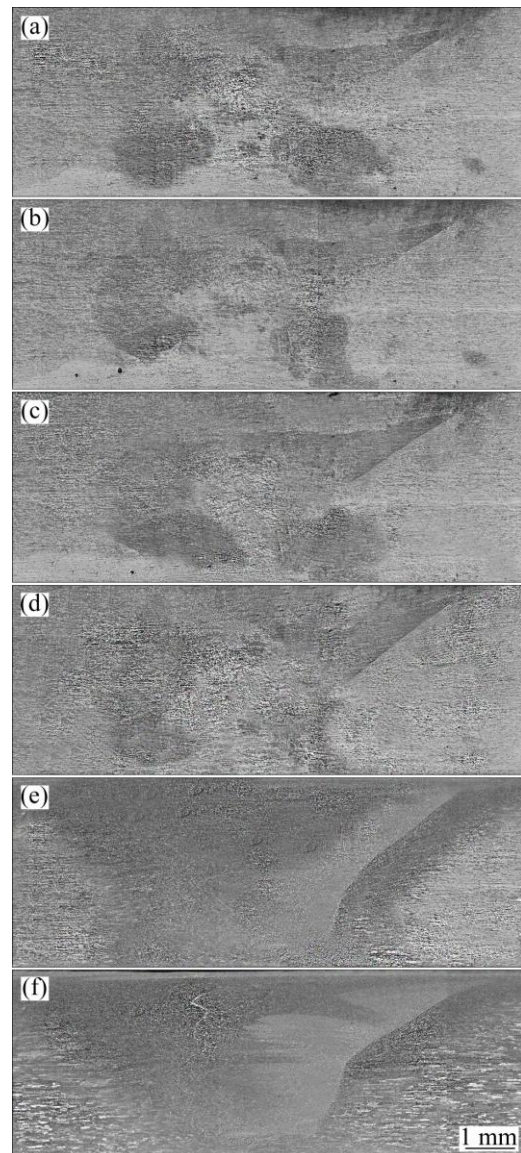


Fig. 3 Macrographs of Sample D50 (a), Sample D65 (b), Sample D75 (c), Sample D85 (d), Sample D95 (e) and Sample S95 (f)

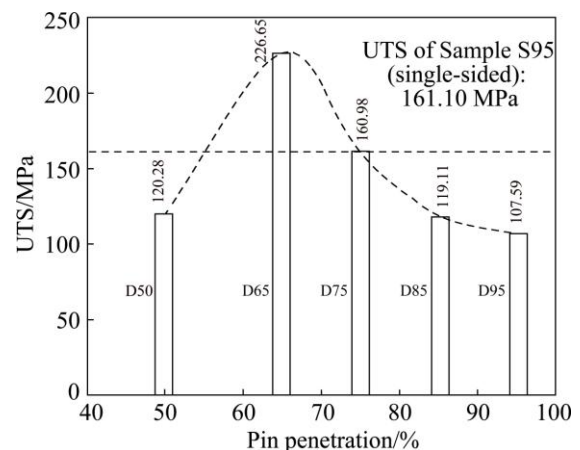


Fig. 4 Ultimate tensile strength of six samples and smooth Bézier spline trend line for Samples D50 to D95

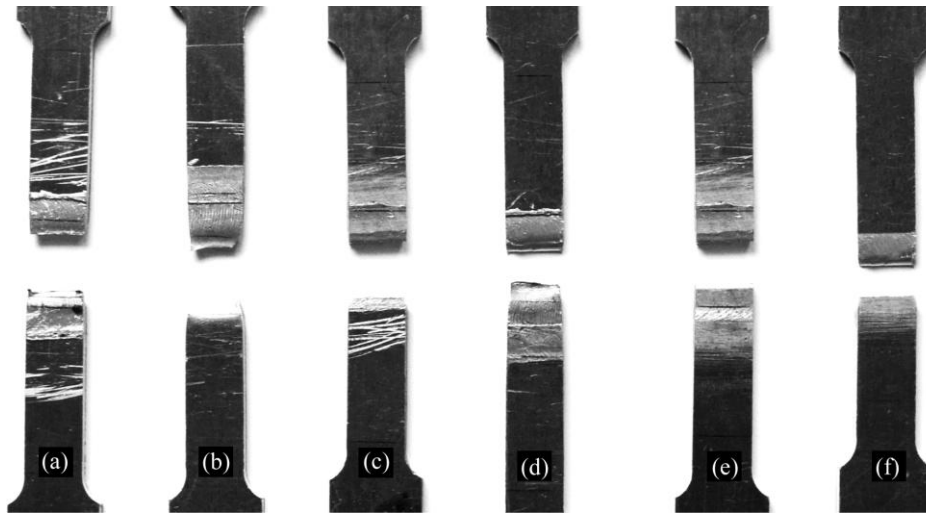


Fig. 5 Different locations of failure: (a) Failure from SZ in Sample D50; (b) Failure from boundaries of TMAZ and HAZ in Sample D65; (c) Failure from boundaries of TMAZ and HAZ in Sample D75; (d) Failure from SZ in Sample D85; (e) Failure from SZ in Sample D95; (f) Failure from boundaries of TMAZ and HAZ in Sample S95

$$Q = \delta Q_{\text{sticking}} + (1 - \delta) Q_{\text{sliding}} \quad (1)$$

where δ is contact state variable. Pure sticking and sliding are defined for values of $\delta=1$ and $\delta=0$, respectively, and the combination of the sticking and sliding is assumed for values of $0 < \delta < 1$. Tool probe side surface heat in sticking and sliding conditions (Q_{ps1} and Q_{ps2}) is calculated using Eqs. (2) and (3), respectively.

$$Q_{\text{ps1}} = \theta \tau \omega \left(\frac{d}{2} \right)^2 H \quad (2)$$

$$Q_{\text{ps2}} = \theta \mu p \omega \left(\frac{d}{2} \right)^2 H \quad (3)$$

where θ is the contact angle between the probe and technological hole, τ is the shear stress of the weld pieces, ω is the tool angular rotation speed, d is the probe tip diameter, μ is the friction coefficient between tool and weld pieces, p is the contact pressure between tool and weld piece, and H is the probe side height plus depth of the shoulder (if applicable). According to Eqs. (2) and (3), heat generated in both sticking and sliding conditions is the function of tool probe height (H). Considering all variables, other than H , to be constants, increasing H results in increasing Q_{ps} , and consequently, due to more heat generated, grain growth occurs. Moreover, since heat is applied from both sides, double-sided welds affect grain size more obviously than single-sided welds. These demonstrate that energy has a considerable impact on the microstructure and joint strength of double-sided AA6061 welds.

Figure 7 represents the macrostructure of the double-sided FS welded AA6061-T913 joint with 15% pass-overlap (Sample D65). At the center of each side, it

is possible to identify the weld SZ. The TMAZ delimited by the dashed lines. After the TMAZ, the HAZ appears. In this welded sample, at the center, a “mix zone” is specified. In this area, both sides of SZ are well mixed which guarantees the passes to meet each other. Due to heat generated from welding of the second side, grain growth has occurred in the first side, and more precipitations have been dissolved probably. Therefore, SZ and TMAZ boundaries at the first side became blurred.

Despite less heat input and mean grain size, Sample D50 showed lower UTS and mechanical properties. A poor “mix zone” can be obtained using an inappropriate pin length. Thus, Sample D50 has not quite enough pin length to make sound and simultaneously mechanically strong welds, and as above mentioned, its failure took place in SZ.

The Vickers microhardness profile of Sample D65 is shown in Fig. 8. In this weld, the hardness of the SZ is slightly higher than that of the TMAZ. The higher hardness values are recognized in SZ compared with TMAZ and HAZ due to finer grains in SZ. The minimum hardness is obtained for the TMAZ. Indeed, softening occurred in the weld zone, and the low hardness plateau extended to the fine-grained area of SZ. These results suggest that dissolution of precipitates has probably occurred in SZ and TMAZ, and, therefore, has led to the softening. The lower hardness observed in HAZ compared with the base metal is believed to be due to over aging occurring in HAZ during the FSW process.

Failure mode of the weld, determined by examination of the fracture surface, is an important index to evaluate the quality of the FSW welds. It is well

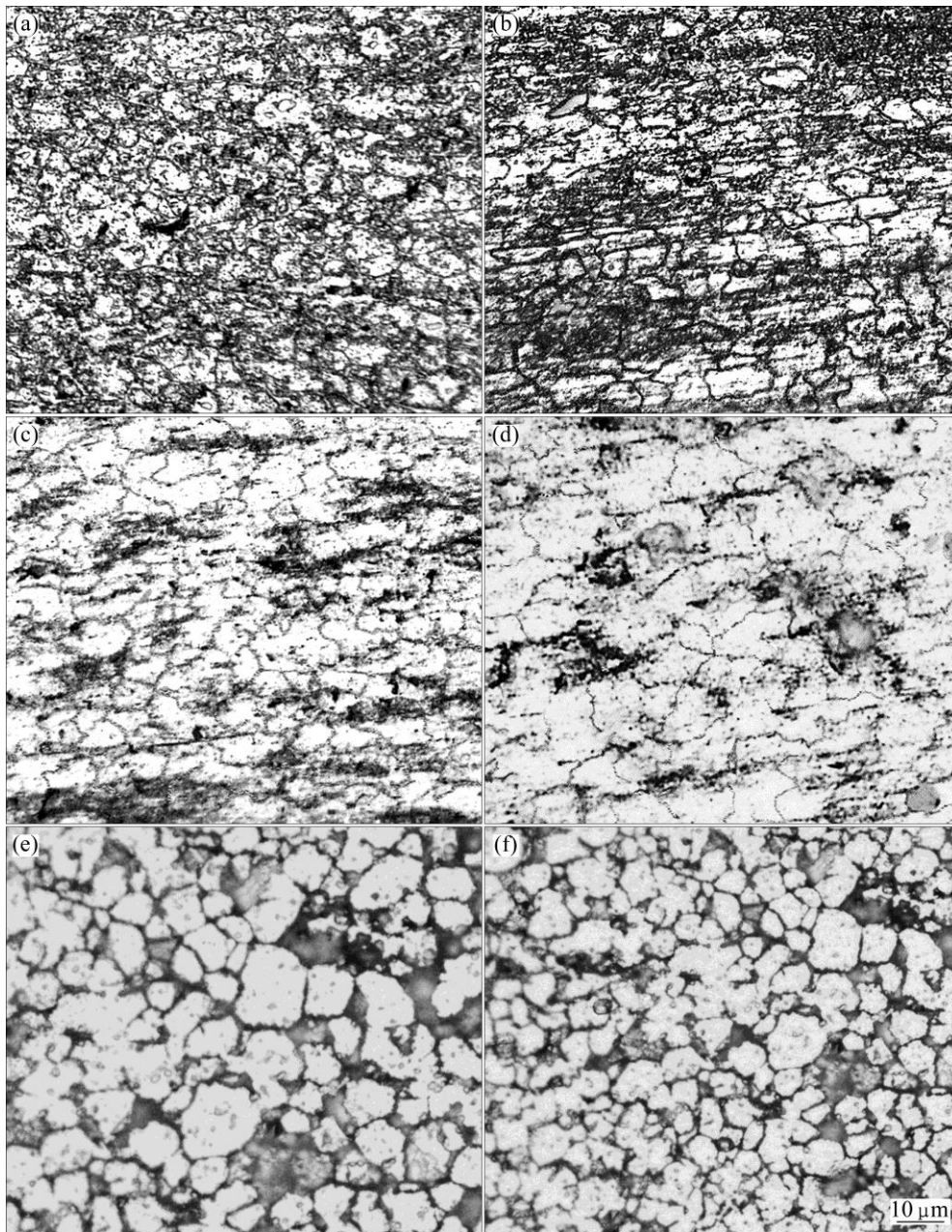


Fig. 6 Microstructures of stir zone for different samples: (a) Sample D50 (mean grain size of $\sim 2.1 \mu\text{m}$); (b) Sample D65 (mean grain size of $\sim 4.5 \mu\text{m}$); (c) Sample D75 (mean grain size of $\sim 5.2 \mu\text{m}$); (d) Sample D85 (mean grain size of $\sim 7.9 \mu\text{m}$); (e) Sample D95 (mean grain size of $\sim 8.3 \mu\text{m}$); (f) Sample S95 (mean grain size of $\sim 2.4 \mu\text{m}$)

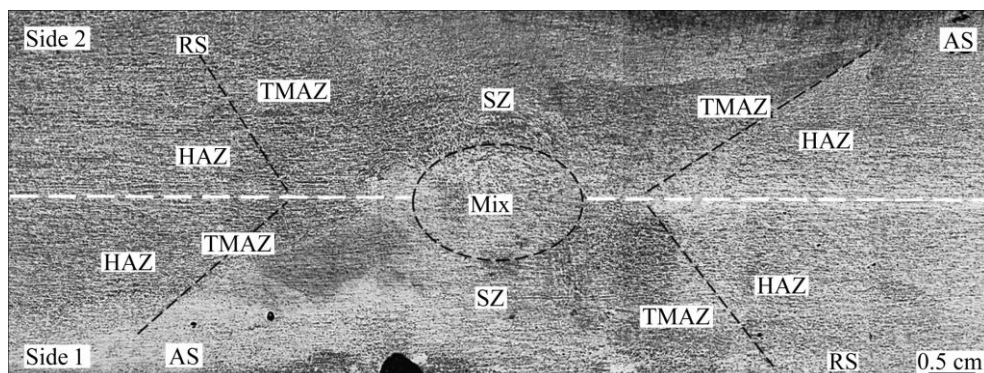


Fig. 7 Macrograph of joint cross-section for Sample D65

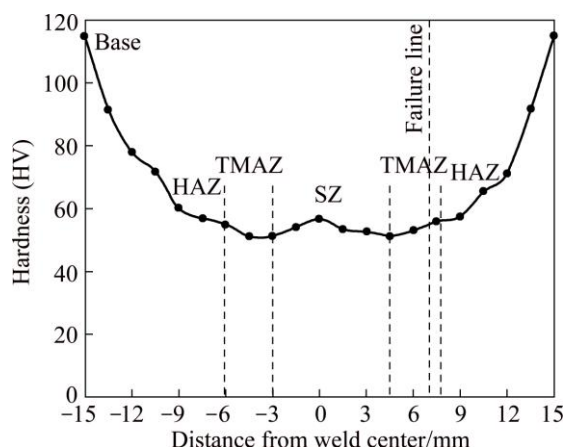


Fig. 8 Microhardness profile of Sample D65 along transverse cross-section of weld fabricated at optimum pin length of 2.6 mm

known that the necking phenomenon occurs in the region with lower hardness; due to its lower resistance to plastic deformation [20]. According to Fig. 8, TMAZ has lower hardness value in comparison with the other regions. In

most cases, the tensile properties and fracture locations of the joints are related to the hardness profiles and the welding defects in the joints [21]. Therefore, it is most likely that the cracks nucleate in the TMAZ, which has the lowest hardness. Figure 9 illustrates the SEM images of fracture surfaces for the FS welded samples. It confirms the presence of dimples, which are characteristics of ductile fracture.

4 Conclusions

- 1) Double-sided friction stir welding of AA6061-T913 sheets at different pin lengths (50%, 65%, 75%, 85% and 95% of the sheet thickness) was investigated.
- 2) Using double-sided FSW in specific ranges of parameters, the mechanical properties of the joints can be improved in comparison with conventional single-sided FSW.
- 3) Increasing pin length caused the grain size of the stir zone to increase, due to more heat generated accompanying with larger pin length.

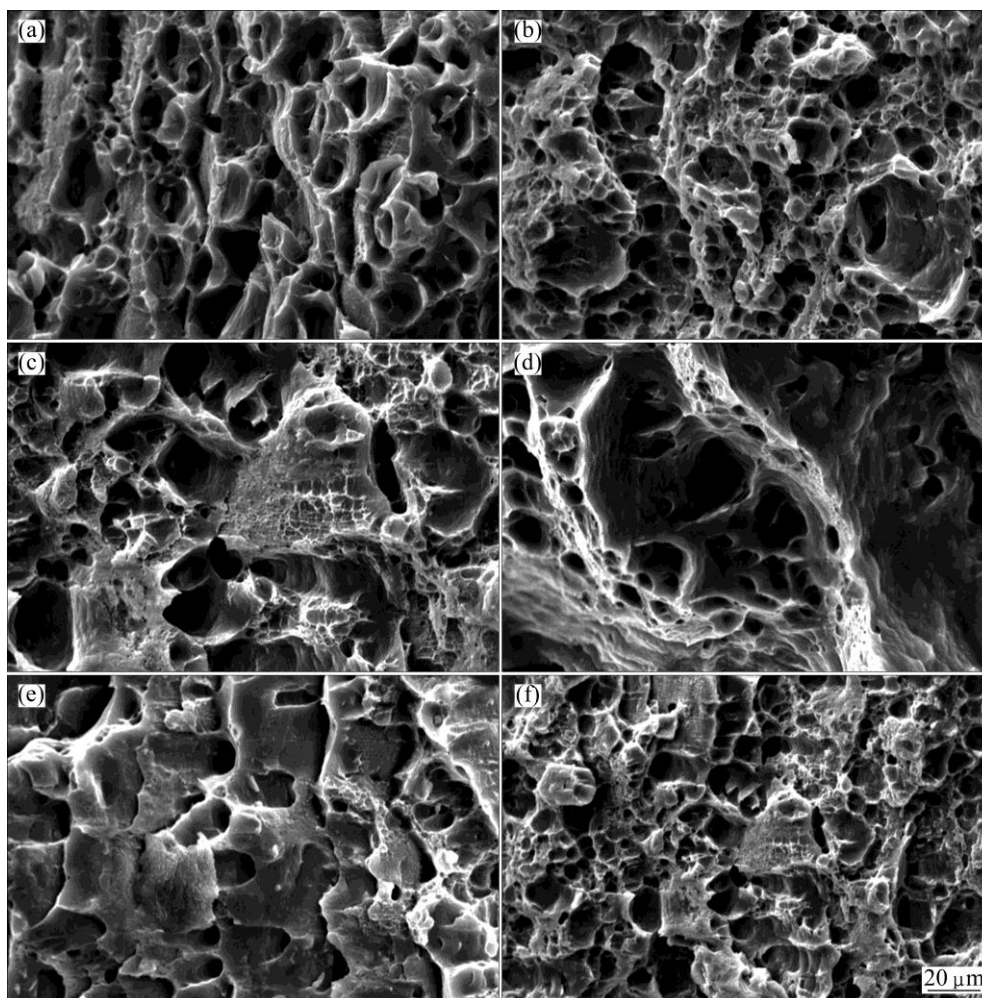


Fig. 9 SEM images of fracture surfaces for different samples: (a) Sample D50; (b) Sample D65; (c) Sample D75; (d) Sample D85; (e) Sample D95; (f) Sample S95

4) The application of a pin length equal to half-thickness of the parent metal causes the bonding between the welds made from both sides to be poor, and it results in a low tensile strength joint (~120 MPa). However, double-sided FSW using a pin length equal to 65% of the parent metal thickness generates the highest UTS (226.6 MPa), which is 41% greater than that obtained for the single-sided FSW joint.

5) The fracture location of the joints is significantly affected by the pin length. The sample welded using a pin length equal to 65% thickness of the parent metal failed from TMAZ. As the pin length increased, fracture location of the joints progressively moved toward SZ.

6) The minimum hardness measured in Sample D65 belonged to the TMAZ (its failure location in tensile test), which had a larger grain size compared with the SZ. Also, it seems that the dissolution of precipitates in the SZ and TMAZ caused them to be softened.

7) The results showed the occurrence of ductile fracture in tensile testing of the double-sided welds.

Acknowledgments

The support of Iran National Science Foundation (INSF) (Grant No. 91051732) is gratefully acknowledged. Also, the authors wish to thank Institute of Iranian National Standards Organization-Mechanical and Metallurgy Research Center and Mr. Derayati for the preparation of project facilities.

References

- [1] LEON J S, JAYAKUMAR V. Investigation of mechanical properties of aluminium 6061 alloy friction stir welding [J]. *American Journal of Mechanical Engineering and Automation*, 2014, 1(1): 6–9.
- [2] FADAEIFARD F, MATORI K A, TOOZANDEHJANI M, DAUD A R, ARIFFIN M, OTHMAN N K. Influence of rotational speed on mechanical properties of friction stir lap welded 6061-T6 Al alloy [J]. *Transactions of Nonferrous Metals Society of China*, 2014, 24(3): 1004–1111.
- [3] MISHRA R S, MA Z Y. Friction stir welding and processing [J]. *Materials Science and Engineering R: Reports*, 2005, 50: 1–78.
- [4] THOMAS W M, NICHOLAS E D, NEEDHAM J C, CHURCH M G, TEMPLESMITH P, DAWES C J. Friction stir welding: G.B. (Great Britain) Patent, 9125978.8 [P]. 1991–04–28.
- [5] ABNAR B, KAZEMINEZHAD M, KOKABI A. Effects of heat input in friction stir welding on microstructure and mechanical properties of AA3003-H18 plates [J]. *Transactions of Nonferrous Metals Society of China*, 2015, 25(7): 2147–2155.
- [6] RAJAKUMAR S, MURALIDHARAN C, BALASUBRAMANIAN V. Establishing empirical relationships to predict grain size and tensile strength of friction stir welded AA 6061-T6 aluminium alloy joints [J]. *Transactions of Nonferrous Metals Society of China*, 2010, 20(10): 1863–1872.
- [7] KUMAR A R, VARGHESE S, SIVAPRAGASH M. A comparative study of the mechanical properties of single and double sided friction stir welded aluminium joints [J]. *Procedia Engineering*, 2012, 38: 3951–3961.
- [8] ABDELRAHMAN M A, GHONEIM M M, ABDELAZIM M E, EL-KOUSS M M R, ABDELRAHEEM N A. The effect of FSW tool geometry on AA6061-T6 weldments [J]. *Arab Journal of Nuclear Sciences and Applications*, 2012, 43: 407–418.
- [9] ROHILLA P, KUMAR N. Experimental investigation of tool geometry on mechanical properties of friction stir welding of AA6061 [J]. *International Journal of Innovative Technology and Exploring Engineering*, 2013, 3: 56–61.
- [10] BISHNOI R N, SAPRA P K, BHAMBHU R. Effect of tool pin profile on mechanical properties of single and double sided friction stir welded aluminium alloy AA19000 [J]. *International Journal of Current Engineering and Technology*, 2013, 3: 1338–1441.
- [11] SINGH Y, SINGH B. Tensile behaviour for aluminium alloy (6061) in single & double pass friction stir welding by using different tool shapes [J]. *International Journal of Research in Engineering and Applied Sciences*, 2014, 4: 43–50.
- [12] CAMPANELLI G C L, CASAVOLA C, MORAMARCO V. Analysis and comparison of friction stir welding and laser assisted friction stir welding of aluminum alloy [J]. *Materials*, 2013, 6: 5923–5941.
- [13] American Society for Testing Materials. ASTM E8/E8M–13a. Standard test methods for tension testing of metallic materials [S]. West Conshohocken, PA: ASTM International, 2013.
- [14] American Society for Testing Materials. ASTM E384–11e1. Standard test method for Knoop and Vickers hardness of materials [S]. West Conshohocken, PA: ASTM International, 2011.
- [15] American Society for Testing Materials. ASTM E3–01. Standard practice for preparation of metallographic specimens [S]. West Conshohocken, PA: ASTM International, 2001.
- [16] American Society for Testing Materials. ASTM E112–13. Standard test methods for determining average grain size [S]. West Conshohocken, PA: ASTM International, 2013.
- [17] DAS H, CHAKRABORTY D, KUMAR PAL T. High-cycle fatigue behavior of friction stir butt welded 6061 aluminium alloy [J]. *Transactions of Nonferrous Metals Society of China*, 2014, 24(3): 648–656.
- [18] GAN W O K, HIRANA S, CHUNG K, KIM C, WAGONER R H. Properties of aluminum alloys 6111 and 5083 [J]. *J Eng Mater Technol*, 2008, 130: 031007.
- [19] ĐURĐANOVIĆ M B, MIJAJLOVIĆ M M, MILČIĆ D S, STAMENKOVIĆ D S. Heat generation during friction stir welding process [J]. *Tribology in Industry*, 2009, 31: 8–14.
- [20] ALIZADEH-SH M, FALSAFI F, MASOUMI M, MARASHI S P H, POURANVARI M. Laser spot welding of AISI 304L: Metallurgical and mechanical properties [J]. *Ironmaking & Steelmaking*, 2014, 41: 161–165.
- [21] LIU H J, CHEN Y C, FENG J C. Effect of heat treatment on tensile properties of friction stir welded joints of 2219-T6 aluminium alloy [J]. *Materials Science and Technology*, 2006, 22: 237–241.

摩擦搅拌针插入深度对双面搅拌摩擦焊 AA6061-T913 铝合金焊接接头的影响

Iman HEJAZI, Seyyed Ehsan MIRSALEHI

Department of Mining and Metallurgical Engineering, Amirkabir University of Technology (Tehran Polytechnic),
424 Hafez Ave, P. O. Box 15875-4413, Tehran, Iran

摘 要: 铝合金搅拌摩擦焊已应用于多个工业领域。搅拌摩擦焊的焊接接头须具有优异的弹塑性及与基体金属相似的变形性能。在本研究中,将双面搅拌摩擦焊与传统的单面板进行对比。采用具有不同搅拌针长度(搅拌针长度为合金板厚度的 50%~95%)的可调节工具对合金板材进行双面搅拌摩擦焊。研究焊接接头的宏观、微观形貌,强度和硬度以确定搅拌针的最佳插入深度。结果表明,当搅拌针长度为合金板厚度的 65%时,双面搅拌摩擦焊焊接接头的极限抗拉强度比单面搅拌摩擦焊接接头的极限抗拉强度提高了 41%。

关键词: AA6061 铝合金; 搅拌摩擦焊; 双面接头; 摩擦搅拌针长度; 力学性能; 显微组织

(Edited by Wei-ping CHEN)